STUDIES ON THE PERMEATION OF HYDROGEN THROUGH STEAM GENERATOR TUBES AT HIGH TEMPERATURES USING AN ELECTROCHEMICAL METHOD

F. Giraudeau

ABSTRACT

The permeation of hydrogen through steam generator tubes at high temperatures (~ 300 °C) has been studied using an electrochemical technique. With this technique, hydrogen is generated on one side of the tube and monitored on the other side. The time for the hydrogen to reach the other side is used to determine the diffusion coefficient of hydrogen in the tube. Boundary conditions at the entry and exit sides have been investigated separately. Preliminary studies were performed on Stainless Steel 316 and Nickel Alloy 800 to better understand the influence of the solution chemistry on the electrochemical evolution of hydrogen. The surface phenomena effect and the trapping effect are discussed to account for differences observed in the permeation response.

The hydrogen permeation through oxides at the exit side has been studied. Two nickel alloys (Alloy 800 and Alloy 600), materials widely used for steam generator tubes, have been investigated. The tubes were prefilmed using two different treatments. The oxides were formed in dry air at high temperatures (300 °C to 600 °C), or in humid gas at 300 °C. The diffusion coefficients at 300 °C in Stainless Steel 316 and Alloy 800 were determined to be of the order of 10^{-6} - 10^{-7} cm^2/s for the bare metal. This is in agreement with results obtained by gas phase permeation techniques in the literature.

L. Yang, F.R. Steward, O de Bouvier

STUDIES ON THE PERMEATION OF HYDROGEN THROUGH STEAM GENERATOR TUBES AT HIGH TEMPERATURES USING AN ELECTROCHEMICAL METHOD

F. Giraudeau, L. Yang, F.R. Steward, O. de Bouvier

1. INTRODUCTION

To suppress the radiolysis of water and control corrosion in the Primary Heat Transport System (PHTS), PWRs (Pressurized Water Reactors) and CANDUs have generally adopted hydrogen water chemistry. To maintain this condition, hydrogen is either continuously or periodically added to the PHTS. Hydrogen isotopes are therefore present and may be a source of contamination. Tritium has been detected in the secondary coolant of nuclear plants. Permeation through steam generator tubes is a possible path for this tritium. Alloy 600 has been proven to crack from both the primary and secondary side during twenty years of experience [1] and hydrogen-assisted cracking has been suggested [2]. Hydrogen diffuses as atoms in metals and the overall process of hydrogen permeation involves complex electrochemical reactions.

Gas permeation through different nickel alloy membranes has been extensively studied [3-9]. However, to our knowledge, no such permeation rate was measured for a liquid phase using an electrochemical method at high temperature. The rate of permeation of hydrogen through steam generator tubes can be different from that measured for gas phase systems due to the passivation of the tube surface by corrosion [10-14]. The thickness, nature and history of the oxide layers influence the hydrogen permeation rate. However, the permeation of hydrogen through oxides at elevated temperatures has been controversial regarding whether or not there is a partial or total reduction of the oxide layer [12, 14-17] in contact with the gas phase.

This paper identifies the parameters controlling the electrochemical permeation of hydrogen in various alloys, particularly Alloy 800.

2. EXPERIMENTAL

2.1. Material

Three nickel alloys were studied: Alloy 800, Alloy 600 and SS316. The chemical composition of each alloy is given in the following table:

Alloy	%C	%Mn	%Si	%Cr	%Ni	%Fe	%Ti	%Cu	%Al	%Mo	%P	%Co	%N
800	0.018	0.68	0.16	21.2	32.3	44.6	0.52	0.05	0.19				
SS316	0.015	1.6	0.54	16.85	12.43	66.0		0.43		2.05	0.025	0.07	0.012
600	0.018	0.77	0.34	16.8	72.4	9.01		0.01		0.01		0.014	0.015

Pieces of 6.35 mm od tubing were used as test material. The wall thicknesses of the Alloy 800 and Alloy 600 were 0.889 mm, while the wall thickness of the SS316 was 1.245 mm.

2.2. Permeation experiments

A hydrogen permeation probe (Fig. 1) was installed in a recirculating loop [18]. The concentrations of boric acid and lithium hydroxide were selected to simulate PWR (or CANDU) coolant chemistry. The primary coolant flowed in the outer shell which was anodically polarized. The carrier gas circulated inside the inner tube which was cathodically polarized using a galvanostatic method (0.025 to 50 mA/cm^2). A constant current was applied between the anode and the cathode with a power supply. The outer and inner tubes were electrically isolated using CONAX fittings EG-250 with the corresponding ceramic insulators and lava seals. The hydrogen permeated from the outer surface to the inner surface of the inner tube sample at 300 °C.

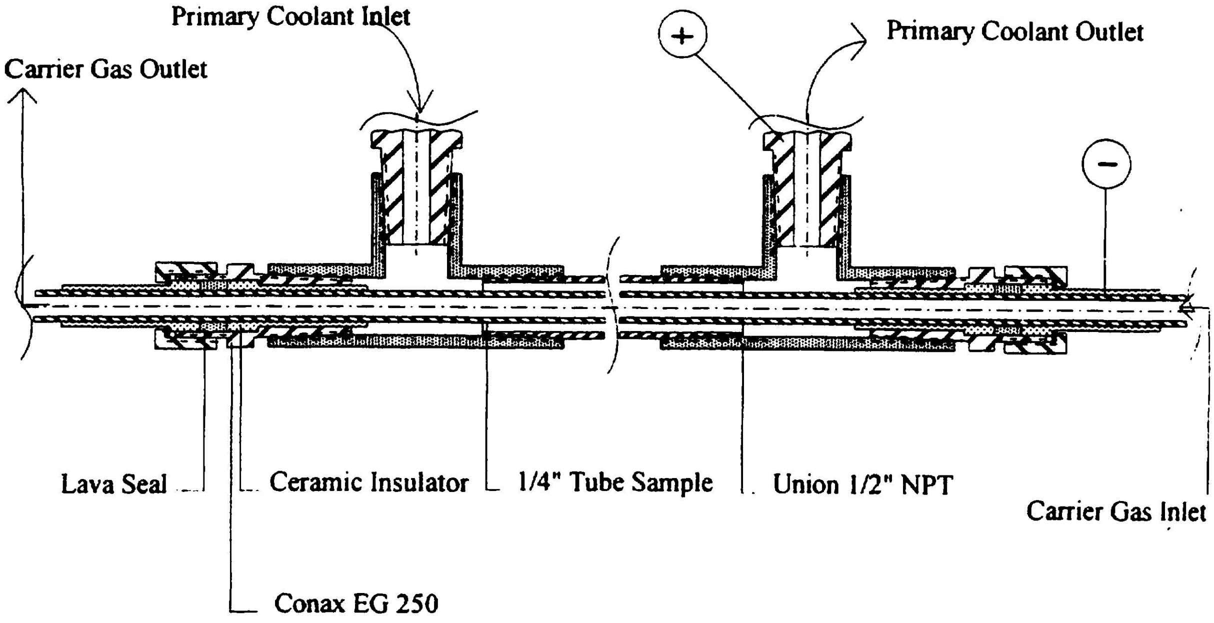

Fig. 1:Electrochemical Hydrogen Permeation Assembly

The gas line (carrier gas at atmospheric pressure) to the gas chromatograph, where the hydrogen was analyzed, was 7 m long and the tube was of 3.175 mm OD SS304. The residence time of the gas in the tube was calculated to be 3.25 min for a flow rate of 2.9 ml/min. This can be considered as negligible in comparison to the measured time-lag, within experimental errors. The inner tube was electrically isolated from the experimental set-up using plastic fittings. Water vapor and oxygen (mainly from the ingress of air through plastic) may oxidize the inner surface of the inner tube at high temperatures. Therefore, a purifier was installed upstream of the tube sample, after the plastic fittings so that oxygen and water from the carrier gas were reduced. However, lithium hydride, which was the reacting species of the purifier, produces hydrogen. The resulting hydrogen baseline was carefully monitored. Argon was chosen as the carrier gas to increase the sensitivity of the TCD filament of the gas chromatograph for hydrogen. Hydrogen atoms were generated on the outer surface of the inner tube. Recombination and release into the primary coolant was the main path for the produced hydrogen. The permeating atomic hydrogen recombined at the inner surface of the inner tube. An Orbisphere analyzer, Model 3600, and the gas chromatograph recorded the levels of hydrogen in the primary coolant and in the gas stream respectively.

2.3. Rising transients

The current was turned on when the baseline was stable. The increasing permeating hydrogen was recorded by the gas chromatograph every 16-17 min until a steady-state was reached. A rising transient was obtained as a function of time. The current was turned off to permit the atomic hydrogen to deplete from the tube sample at the working temperature. Successive rising transients were produced by repeating the above procedure.

2.4. Surface preparation

The tube samples were prepared by circulating a 1M nitric acid solution inside the tube overnight. The tubes were then rinsed with acetone and dried with compressed air. This procedure was followed to perform a standard cleaning of the tube.

In order to study the effect of oxides on the rising transients, the tubes were prefilmed under specific conditions. Two methods were used: ambient air at 600 °C, and humid gas at 300 °C with a duration from 24 to 48 hrs. The prefilming in air was carried out in a furnace before the run whereas the prefilming in humid gas was performed on-line by bubbling argon or air through a solution (various concentrations of boric acid and/or lithium hydroxide) at a fixed temperature to obtain a certain level of humidity. The wet gas was introduced upstream of the sample tube in order to prefilm the inner surface. During prefilming, the gas purifier upstream of the sample tube was by-passed. When the surface conditioning was finished, the purifier was returned in-line. The current was turned on either 15 min or 2 to 3 hrs after the end of the prefilming process.

2.5. Data processing

Data were collected using two computers. A Varian Model 3600 gas chromatograph was connected to a computer workstation using Varian Star 4.0 software for the gas composition analysis. Temperature, Orbisphere voltage and potential between the tubes of the electrochemical assembly were measured every 5 min using Keithley meters connected to a computer through an IEEE interface card.

Apparent diffusion coefficients were computed from the rising transients using the time-lag method. The total amount of hydrogen which has diffused out of the tube from the time when the current is turned on (integration of the rising transient between time 0 and t) increases linearly with time when the steady-state is reached. The intercept of the straight line with the time-axis gives the time-lag. Known boundary conditions are required to determine the hydrogen concentration profile through the tube wall and the time-lag as a function of the apparent diffusivity. These were calculated for the galvanostatic boundaries (constant hydrogen flux on the cathodic surface) using Laplace transforms. Jaeger [19] found a similar expression corresponding to potentiostatic boundaries (constant hydrogen concentration on the cathodic surface) for the tube shape.

3. RESULTS AND DISCUSSIONS

3.1. Surface Effects on the Cathodic Side (entry side)

The overall process of electrochemical permeation of hydrogen through metals is presented in Fig.2. The cathodic side (outer surface of the tube) is modelled for an acid environment where the hydrogen ion is reduced to produce atomic hydrogen (step II). However, for a basic pH, steps I and II do not apply. In this case, water combines with electrons to produce atomic hydrogen and hydroxide ions ($H_2O + e^- \rightarrow H_{ads} + OH^-$). The latter specie diffuses back to the bulk of the primary coolant. Both electrochemical reactions compete in a range of pH near neutral. This scheme represents what happens at steady-state but does not account for phenomena occuring during the transient period. For example, the partial or total reduction of the oxide that exists prior to the cathodic polarization is not represented. Assuming instantaneous constant

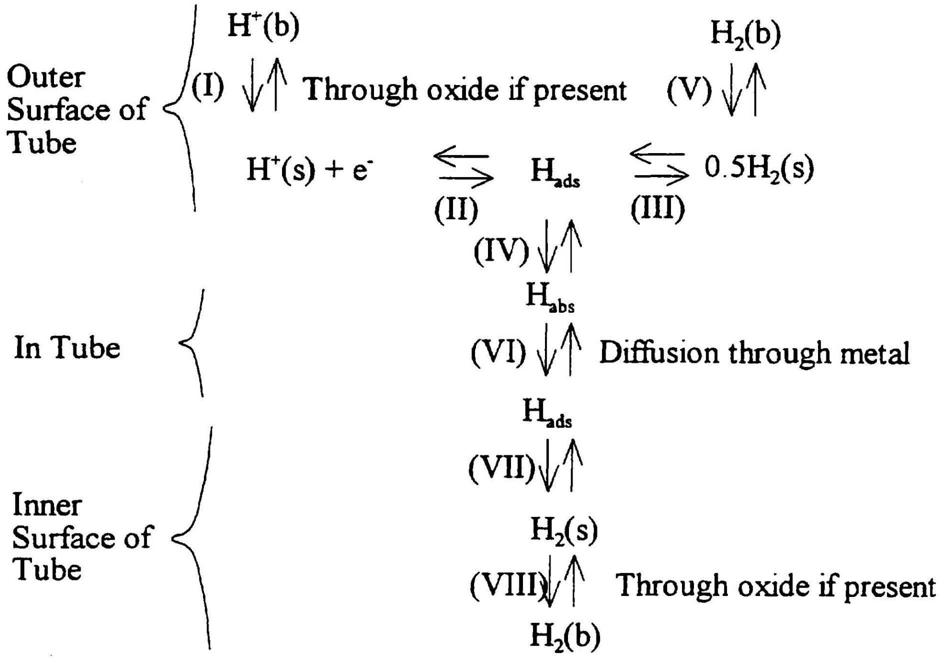

Fig.2: Overall Process of Electrochemical Permeation of Hydrogen Through a Tube Wall. The bulk phase and surface state are represented respectively by (b) and (s), the absorbed and adsorbed states by (abs) and (ads).

boundary conditions may not allow one to correctly interpret experimental results. In order to better understand the surface phenomena, two runs were performed with SS316 and one with Alloy 800. Lithium hydroxide and boric acid concentrations were changed and the pH was measured. Three different gases (argon, hydrogen and air) were studied and the current was varied. Five different pH(25 °C)'s were studied: 3.1, 5.2, 6.0, 7.8 and 11.2. The range of current densities was between 0.025 and 50 mA/cm^2. From the tests carried out, three types of transients were identified as shown in Fig.3. Ideally, the permeating hydrogen flux reaches a steady-state value (Fig.3A). This corresponds to a constant subsurface concentration or flux at the entry side. However, a review of the results obtained has shown that the shapes given in Fig.3B and C can be obtained for a specific pH and current. In alkaline solutions (e.g. pH 11.2), experimental transients of type C were found whereas, in moderate acid solutions (pH 5.2 to 7.8), experimental transients of type A, B and C were found depending on the current density applied. Low current densities led to type B, moderate current densities to type A and high current densities to type C. Finally, acid solutions (pH 3.1) led only to transients of type B.

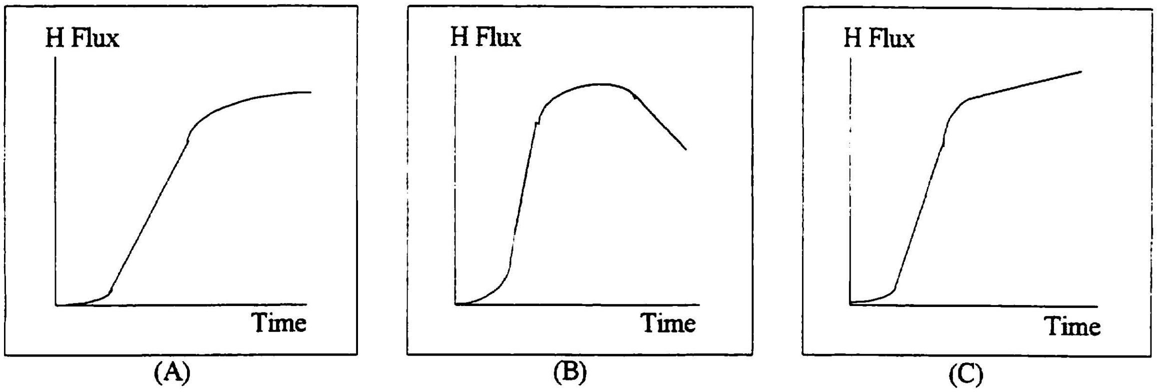

Fig.3: Type of Transients Observed

Pumphrey [21] reviewed experimental results from other authors for low temperature data and showed that step IV sets the boundary condition at the entry side. However, he excluded all transients of type B, as anomalous experimental curves. Chernenko et al. [22] have shown that under some circumstances for the electrochemical permeation of hydrogen at low temperatures the rate controlling step may not be the bulk metal surface or the diffusion through the oxide at the exit side of a palladium membrane. They suggested that the reduction of water in alkaline solution or the diffusion of hydrogen ions to the metal surface in acid solutions may be the limiting steps. However, we measured the rate of the hydrogen evolution and have not found a systematic correlation between the permeating hydrogen transient rates and the hydrogen evolution rates. Boric acid was added as an electrolyte on the cathodic side and acted as a poison of the hydrogen recombination reaction. Further work is needed to study the possible effect of boron on the different shapes obtained. The comparison of experimental curves with the galvanostatic and potentiostatic models, using apparent diffusivity values, has shown that the potentiostatic model is closer to experimental results (Fig.4). Future work includes the modelling of the electrochemical permeation to correlate with the experimental results. Therefore, apparent diffusivities were

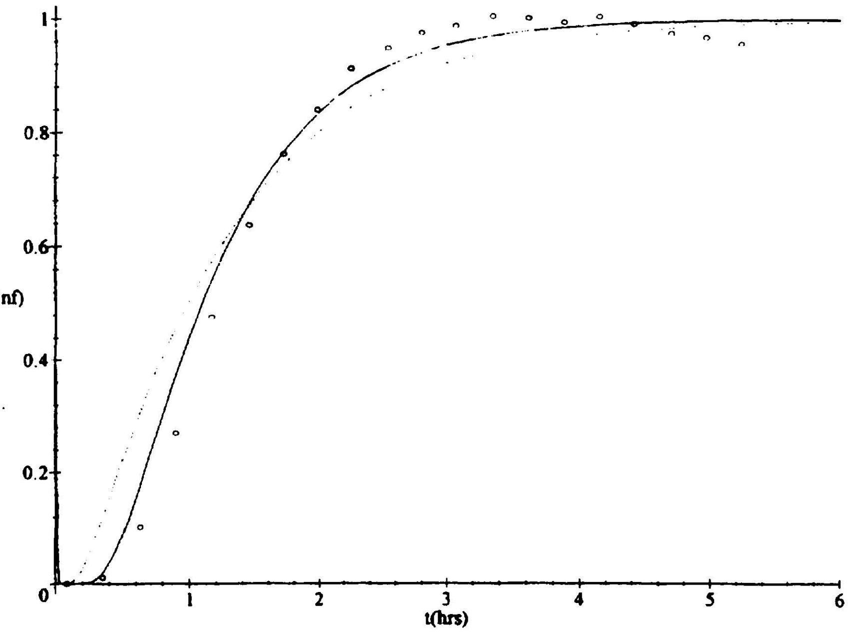

Fig.4: Normalized rising transient. Alloy 800; 307.7 °C; 1 mA/cm^2; pH 3.1; o experimental data, ---: galvanostatic, ___: potentiostatic.

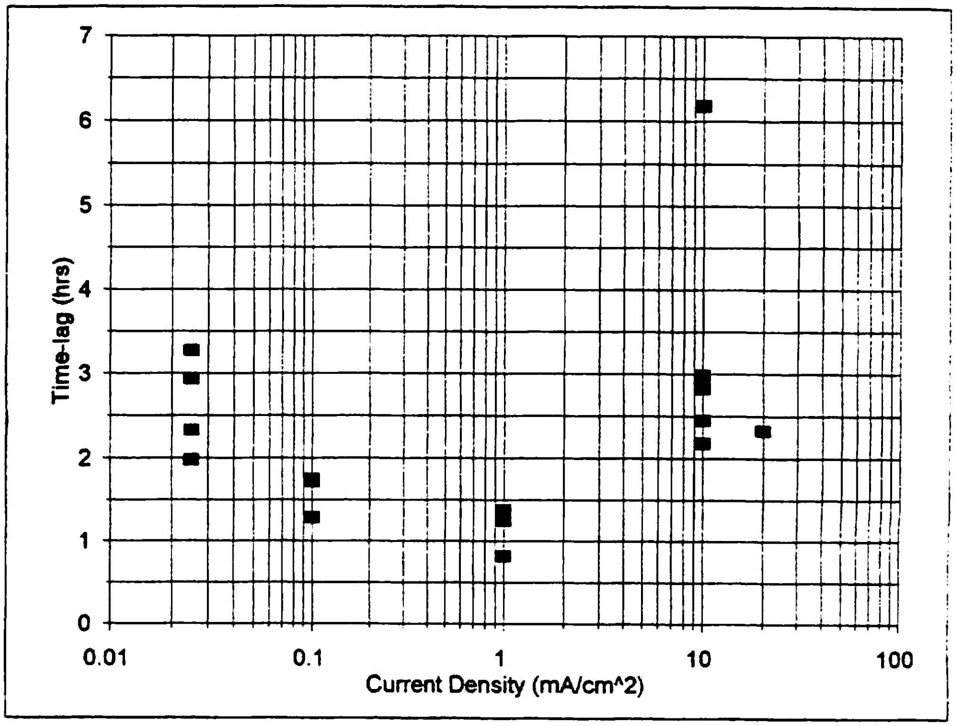

Fig.5: Time-lag versus current density. Alloy 800, 300.6 °C; pH 3.1.

calculated using the potentiostatic time-lag formula. Time-lags could not be calculated for type C transients and the maximum was used to determine time-lags for type B transients.

The current density had an effect on the time-lag (Fig.5). Decreasing currents (0.1 to 0.025 mA/cm^2) led to increasing time-lags because of the partial reduction of the oxide at the entry side. The time-lags obtained for 0.025 mA/cm^2 showed that the longer the time to build up the oxide layer at the entry side (high temperature corrosion), the longer the time delay to partly reduce this oxide layer. Multiple transients were carried out and led to lower values for 0.1 and 1 mA/cm^2. The oxide layer had been partly reduced prior to the current increase. High current densities led to higher time-lags. The trapping phenomena described in the next section could account for these results. Dissolved gases are expected to influence steps I, II, III and V (Fig.1) at the entry side. Oxygen and hydrogen are both produced in situ, respectively at the anode and cathode. It was observed that, as the oxygen concentration increases, the breakthrough time increases. The partial reduction of the oxide which grows between each transient because of corrosion requires a longer time. On the other hand, hydrogen led to time-lags which do not differ significantly from those obtained with argon (inert gas). Increased dissolved oxygen retards the increase of the hydrogen subsurface concentration at the entry side. A permanent oxide layer through which hydrogen ions, H$^+$, diffuse to be reduced at the oxide/metal interface (step I) may account for this observation. After reaching steady-state, oxygen was dissolved (air bubbled in the water tank) and the permeating hydrogen flux was recorded (Fig.6). Approximately two hours after changing the gas, the permeating hydrogen decreases, then increases. The current was stopped before it could reach steady-state. The drop may be explained by oxide growth which slows down the diffusion of hydroxonium ions to the metal surface, followed by an increase due to a lower hydrogen recombination (step III) since hydrogen diffusion through oxide is slow (step V).

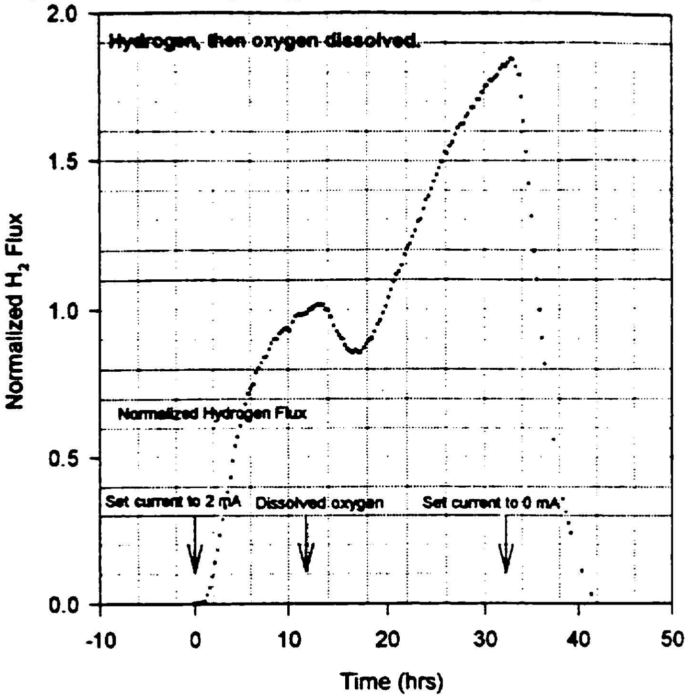

Fig.6: Normalized hydrogen flux, dissolved oxygen effect. SS316, pH 5.2, 0.1 mA/cm^2.

3.2. Temperature dependance

Experiments were performed for Alloy 800 to determine the temperature dependance of the time-lag (i.e. apparent diffusivity, Fig. 7). No data were found in the literature for Alloy 800 over the range of temperatures investigated. However, the composition of alloy GH35A [5] with respect to the main three elements (nickel, chromium and iron) is close to that of Alloy 800. Results obtained in this work are approximately double of those of Xu et al..

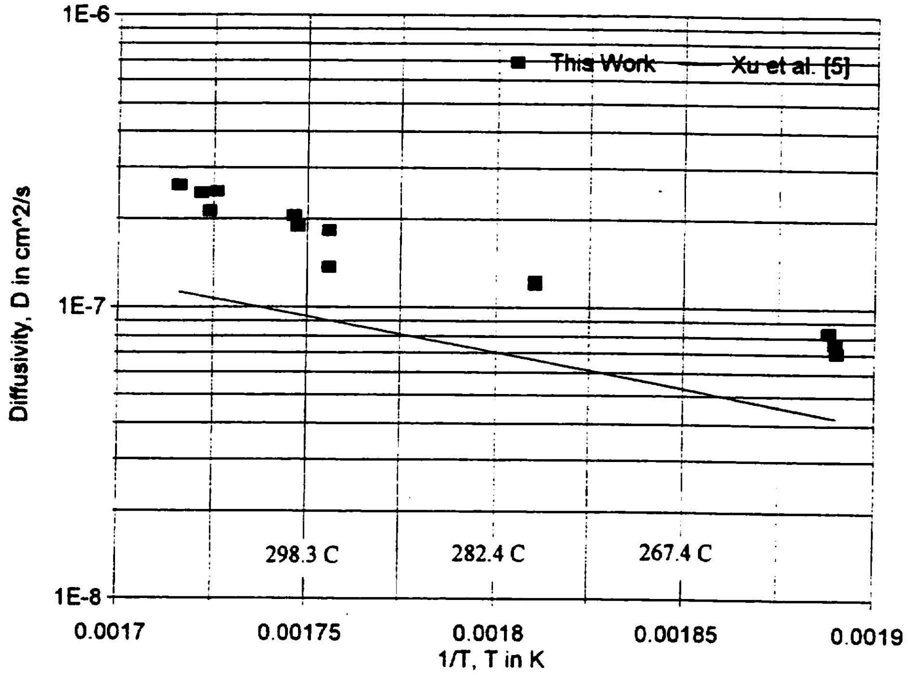

Fig.7: Temperature dependance of the apparent diffusivity for Alloy 800, charging current 20 mA, alloy GH35A for reference [5].

3.3. Trapping

Hydrogen has three types of sites in metals [20]: diffusion sites, reversible sites and irreversible saturable traps. The lattice, or "true", diffusivity is associated with diffusion sites. Reversible sites can be pictured as holes which can be filled or emptied according to local thermodynamic equilibrium (gradient of temperature, concentration or electric field). Irreversible saturable traps may be represented by holes which can be filled but not emptied.

Therefore, hydrogen isotopes may be trapped in the bulk of the metal (e.g. tritium from the primary side coolant in steam generator tubes). Traps may also enhance the risk of cracking (Alloy 600) since hydrogen-assisted cracking has been proposed as the failure mechanism depending on the environment [2].

Reversible traps should abide by the laws of thermodynamic. Thus, this equilibrium is temperature dependant. When the current is turned off, hydrogen is depleted from the metal and the final concentration of hydrogen in the metal is theoretically in equilibrium with the hydrogen

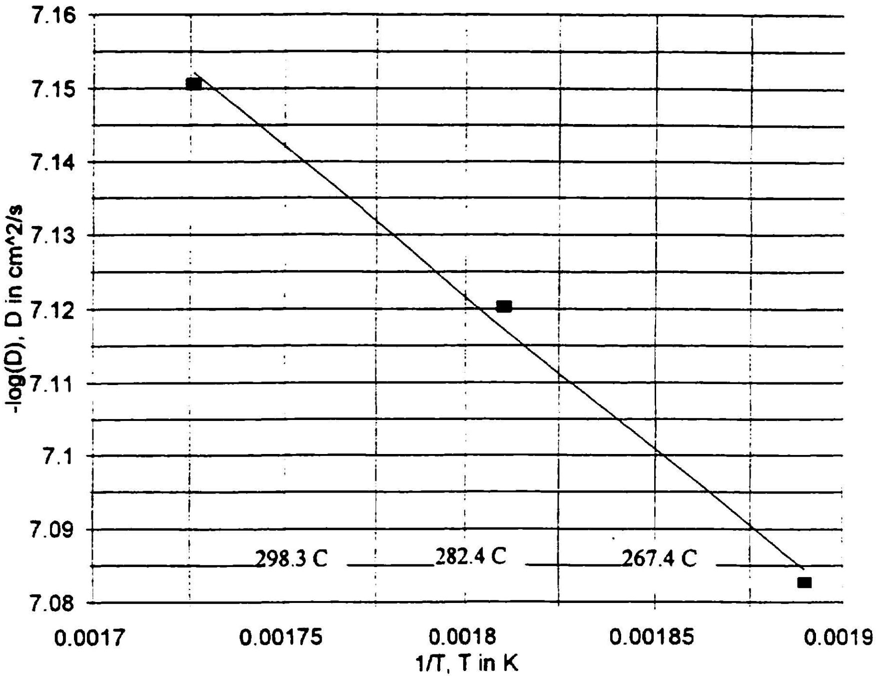

Fig.8: Trapping evidence: apparent diffusivity as a function of temperature of hydrogen depletion, Alloy 800, charging current 20 mA, charging temperature 256 °C.

fugacity of both sides of the tube. Since a protective oxide develops on the outer surface by high temperature corrosion, the hydrogen fugacity in the tube should be in equilibrium with the hydrogen partial pressure in the carrier gas. Hydrogen charging occurred at 256 °C and the desorption took place at different temperatures. Our experimental conditions were set so that this partial pressure can be assumed to be zero. The temperature at which the hydrogen was depleted should not have influenced the apparent diffusivity of the following rising transient. It was observed that, at a constant temperature, the rising transient apparent diffusivity depended on the temperature at which the hydrogen was depleted (Fig.8). Therefore, reversible trapping should be responsible for this phenomenon. Higher current densities increase reversible trapping and may account partly for the results observed for 10-20 mA/cm^2 (Fig.5).

Irreversible trapping is usually identified by comparing the first rising transient with the following rising transients. Traps are filled during the first rising transient and a larger time-lag (lower apparent diffusivity) results for this first rising transient. This characteristic was not clearly observed in this work.

3.4. Surface Effects on the Inner Surface (exit side)

The interest of the present work was to determine the influence of an oxide layer on the exit side. An oxide layer was grown under known conditions (humidity, temperature, nature of gas) in the gas phase and transients were carried out to determine the apparent diffusion coefficient.

Figure 9 presents the rising transients, after the prefilming operation, carried out as single transients. The current was turned on 15 min after the end of the prefilming. As mentioned previously, a constant hydrogen baseline was detected. This figure shows that the baseline drops for the first transient. Hydrogen was adsorbed/absorbed in the oxide layer. On the other hand, the two following rising transients were characterized by a smaller time-lag and a normal hydrogen baseline. Another test was carried out to prove that the entry side oxide could not be accountable for the difference in time-lags observed between the first transient and the two subsequent transients. Consequently, the oxide layer structure on the inner surface of the tube (exit side) in contact with a dry gas phase (argon) had most likely been modified by a high hydrogen flux. Future analysis of the inner surface before and after the first transient should help in understanding the observations made.

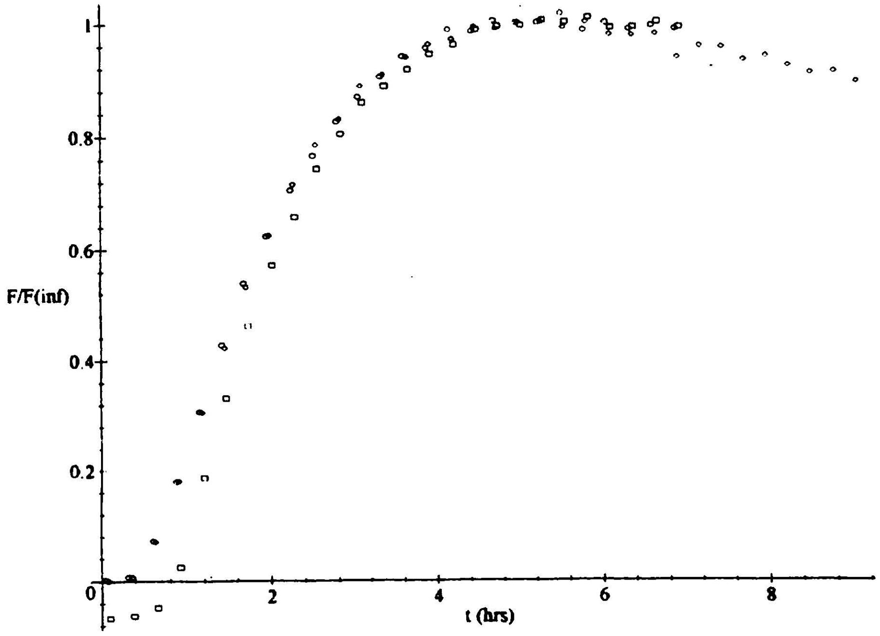

Fig.9: Normalized hydrogen flux as a function of time for the oxide effect evidence on the exit side. Alloy 800; Prefilming for 24 hrs with air bubbled through a 20 ppm lithium solution at room temperature, cathodic current 2 mA; □: Transient 1, ◇: Transient 2, o: Transient 3.

More experiments were performed by varying prefilming conditions at 300 °C but no significant differences were observed from one test to another. Prefilming was also carried out on Alloy 600 at 600 °C in air for one week but, similarly, the oxide appeared to be reduced after the first transient. Prefilming on Alloy 600 at 300 °C in humid air or argon also led to results similar to those for Alloy 800. The apparent diffusivity values at 300 °C were calculated to be in the same range of values as for Alloy 800. A few rising transients were also obtained with a high humidity air/argon gas mixture as a carrier gas. By varying the oxygen percentage from 0 to 4000-5000 ppmv, permeating hydrogen was found to react partly with oxygen. Consequently, the time-lag values calculated were larger than with pure dry argon but the oxide layer did not account for the difference in time-lag since the steady-state values were comparable, taking into account the reaction between oxygen and permeating hydrogen.

Experiments with a circulating secondary coolant have been started to study the permeation through an oxide layer in liquid phase.

4. CONCLUSIONS

The electrochemical permeation of hydrogen through steam generator Alloy 800 and 600 was studied. Three main phenomena were investigated and some conclusions can be drawn:

1- The shape of the transient is related to the pH and current density. The addition of boric acid as an electrolyte to poison the recombination of hydrogen on the cathodic side may have an effect on the phenomenon observed.
2- There is an initial jump in hydrogen subsurface concentration when the current is turned on since the permeating hydrogen flux fits the potentiostatic model for the first part of the transient.
3- Low current densities lead to higher time-lags because of the time delay imposed by the oxide layer at the entry side.
4- High current densities lead to higher time-lags because of trapping and surface phenomena.
5- Dissolved oxygen promotes the growth of oxide which may hinder the transport of species from the bulk of the solution to the metal and vice-versa.
6- Reversible trapping was identified by studying the temperature dependance of the apparent diffusivity.
7- Oxide layers on metal in contact with the dry gas phase do not hinder the transport or recombination of hydrogen at high temperatures. Their structure is most likely modified by a high flux of hydrogen in such a way that they are ineffective in limiting the permeation of hydrogen.

Transport phenomena in oxides have often been studied through the migration of metal ions (iron, chromium, nickel) and the transport of oxygen but rarely through hydrogen diffusion. Studies with a liquid phase on the exit side should provide valuable data on the corrosion theory of alloys useful for stress corrosion cracking models which involve a hydrogen dependance. Hydrogen permeation rate from the primary side to the secondary side could also be extrapolated from the results obtained which is of interest when considering tritium.

The interest of this study also lies in the selection of alloys. The less permeable its oxide layer(s) is to hydrogen, the more resistant the alloy is to corrosion. On the other hand, the ideal lifetime for a steam generator tube is the life of the nuclear plant (30 to 40 years). Models need to be developped to account for the possible failure of a tube. The present work preceeds high temperature hydrogen permeation studies in the liquid phase which are more relevant than the previous studies in the gas phase or in the liquid phase at low temperatures. Future work also includes modelling of the permeation process.

5. ACKNOWLEDGEMENTS

The authors are thankful to Dr Lister and Ms Sun for valuable discussions.

6. REFERENCES

1. R.B. Rebak and Z. Szklarska-Smialowska, Corr. Sci., Vol. 38, No. 6, 971-988 (1996)
2. A. Turnbull, R.G. Ballinger, I.S. Hwang, M.M. Morra, M. Psaila-Dombrowski and R.M. Gates, Met. Trans. A, Vol. 23A, 3231-3244 (1992)
3. D.J. Mitchell and E.M. Edge, J. Appl. Phys., Vol. 57, No. 12, 5226-5235 (1985)
4. T.-P. Perng, M.J. Johnson and C.J. Altstetter, Metall. Trans. A, Vol. 19A, 1187-1192 (1988)
5. J. Xu, X.K. Sun, W.X. Chen and Y.Y. Li, Acta Metall. Mater., Vol 41, 1455-1459 (1993)
6. J. Xu, X.K. Sun, Q.Q. Liu, X. Zhao and C.G. Fan, Scripta Metall. Mater., Vol. 28, 1251-1256 (1993)
7. J. Xu, X.K. Sun, Q.Q. Liu and W.X. Chen, Metall. Mater. Trans. A - Phys. Metall. Mater. Sci., Vol. 25A, No. 3, 539-544 (1994)
8. W.M. Robertson, Metall. Trans. A, Vol. 8A, 1709-1712 (1977)
9. Y. Yamanishi, T. Tanabe and S. Imoto, Trans. Jpn. Inst. Met., Vol. 24, No. 1, 49-58 (1983)
10. R.A. Strehlow and H.C. Savage, Nucl. Tech., Vol. 22, 127-137 (1974)
11. M.R. Piggot and A.C. Siarkowski, J. Iron and Steel Inst., Vol. 210, 901-905 (1972)
12. T.-P. Perng and C.J. Altstetter, Acta Metall, Vol. 36, No. 5, 1251-1260 (1988)
13. Y. Ishikawa, T. Yoshimura and M. Arai, Vacuum, Vol. 47, No. 6-8, 701-704 (1996)
14. W.A. Swansiger, R.G. Musket, L.J. Weirick and W. Bauer, J. Nucl. Mater., Vol. 53, 307-312 (1974)
15. Y. Ishikawa and T. Yoshimura, J. Vacuum Sci. Tech. A - Vacuum Surfaces and Films, Vol. 13, No. 4, 1847-1852 (1995)
16. P. Bruzzoni and R. Garavaglia, Corr. Sci., Vol. 33, No. 11, 1797-1807 (1992)
17. L. Tomlinson, N.J. Cory, Corr. Sci., Vol. 29, No. 8, 939-965 (1989)
18. F. Giraudeau, "Permeation Loss of Hydrogen in the Primary Heat Transport System Through Steam Generator Tubes", Proposal for Doctorate in Engineering, University of New Brunswick, Fredericton, N.B., 17p. (1996)
19. J.C. Jaeger, Trans. Faraday Soc., Vol. 42, 615-616 (1946)
20. A. Turnbull, M. Saenz de Santa Maria and N.D. Thomas, Corr. Sci., Vol. 29, No. 1, 89-104 (1989)
21. P.H. Pumphrey, Scripta Metall., Vol. 14, No. 7, 695-701 (1980)
22. V.I. Chernenko and T.G. Yakunina, Sov. Electrochem., Vol. 18, 803-807 (1982)